Available online at www.sciencedirect.com
SCIENCE DIRECT®
Journal of Sound and Vibration 278 (2004) 1147–1162
JOURNAL OF SOUND AND VIBRATION
www.elsevier.com/locate/jsvi

Geometric stiffening effect on rigid-flexible coupling dynamics of an elastic beam

J.Y. Liu*, J.Z. Hong

Department of Engineering Mechanics, Shanghai Jiao Tong University, Shanghai 200030, People's Republic of China

Received 20 December 2002; accepted 24 October 2003

Abstract

In the previous work, the authors examined the effect of the geometric stiffness terms on the stability of an elastic beam undergoing prescribed large overall motion. The aim of the present work is to extend the geometrically non-linear formulations to an elastic beam with free large overall motions. The equations of motion are derived taking into account the foreshortening deformation term, therefore, the equations include the geometric mass and force matrices, which have geometric stiffening effect on the rigid-flexible coupling dynamics of the system. The numerical results obtained in this investigation reveal the significant difference between the deformations with and without stiffening effect. Furthermore, the stiffening effect on the large overall motion is investigated. An influence ratio is employed as a criterion to clarify the application range of the conventional linear modelling method, in which the stiffening effect is neglected. The effectiveness of the criterion is examined by two simulation examples.

1. Introduction

In the hybrid co-ordinate formulation of flexible multibody systems, the displacements of each body are partitioned into displacements due to large overall motions and displacements due to deformation. Two sets of co-ordinates are used to identify the configuration of each flexible body: reference and elastic co-ordinates. The reference co-ordinates define the position and orientation of a body reference, and the elastic co-ordinates describe the elastic deformation with respect to the body-fixed co-ordinate system. Using the linear finite element method and modal truncation approach, the deformation of the flexible multibody system can be expressed by a small number of co-ordinates [1,2]. However, in the conventional linear modelling method, the quadratic term in

*Corresponding author. Tel.: +86-21-64224865; fax: +86-21-64182587.
E-mail address: liujy@sjtu.edu.cn (J.Y. Liu).

0022-460X/$ - see front matter
doi:10.1016/j.jsv.2003.10.014

longitudinal deformation, which accounts for the foreshortening effect, is not included in the deformation expressions. It has been shown that such formulation produces erroneous simulation results when the structures undergo large overall motions [3].

In order to solve the problem of the conventional linear modelling method, the geometrically non-linear formulations are put forward in Refs. [4,5]. Due to the large rotations, the non-linear strain–displacement relations are used for deriving the dynamic equations, and the geometric non-linearities are included via the stiffness terms. Since an accurate representation of axial displacement requires the use of large number of axial shape functions if the non-linear stiffness matrices are used, a further improvement in the formulation can be achieved by using an axial co-ordinate along the deformed axis [6–10]. The use of this representation takes into account the foreshortening effect without the need to include high frequency axial modes, and the geometric stiffness terms are included in the equations of motion. In order to clarify the limit of the validity of the conventional modelling method, a criterion on inclusion of stress stiffening effects is put forward in Ref. [11]. In these literatures, only the effect of the geometric stiffness terms on the deformation of the body undergoing prescribed large overall motion is investigated. Recently, dynamic performance of a rotating and translating beam is investigated in Ref. [12], and the coupling between the deformation and the base displacement is revealed. However, with the prescribed rotating speed, the effect of dynamic stiffening on the rotating speed is not taken into account.

The objective of the paper is to extend the geometrically non-linear formulations to an elastic beam with free large overall motions. By using an axial co-ordinate, the foreshortening deformation is included in the longitudinal deformation. The modal assumption method is used for discretization and the equations of motion of an elastic beam are derived based on virtual work principle. The influence of the geometric force and mass matrices on the rigid-flexible coupling dynamics of the system is investigated. An influence ratio is defined to clarify the limit of the validity of the conventional linear model.

2. Kinematics of an elastic beam

In this section, a dynamic model of an elastic beam is established based on the following assumptions. The beam is homogeneous and isotropic, and the effects due to eccentricity are not considered. The beam has a slender shape so that the shear and rotary inertia effects are neglected.

Consider the elastic beam undergoing free large overall motions as shown in Fig. 1. To describe the motion of the beam, two co-ordinate systems are introduced. O_0–$X_0Y_0Z_0$ is the global co-ordinate system, and O_1–$X_1Y_1Z_1$ is the body-fixed frame. The position vector of an arbitrary point on the central line of the elastic beam can be defined with respect to O_0–$X_0Y_0Z_0$ as

$$\vec{r} = \vec{r}_0 + \vec{\rho}, \tag{1}$$

where

$$\vec{\rho} = \vec{\rho}_0 + \vec{u}, \tag{2}$$

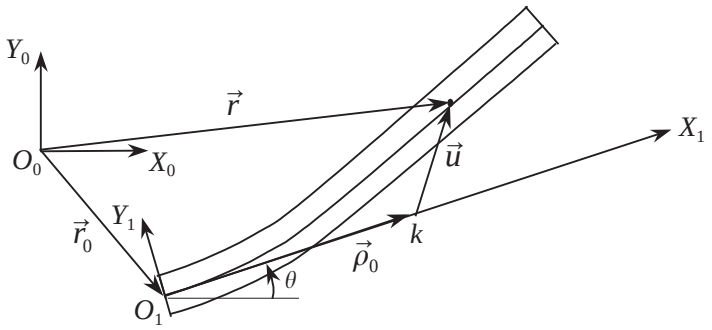

Fig. 1. Elastic beam with free large overall motions.

and, as shown in Fig. 1, $\vec{r}_0$ is the position vector of the reference point O_1, $\vec{\rho}_0$ is the position vector of the arbitrary point with respect to O_1–$X_1Y_1Z_1$ in the undeformed state, and $\vec{u}$ is the deformation vector.

3. Description of deformation

Considering the foreshortening deformation, the longitudinal deformation of the arbitrary point on the central line can be written as [8]

$$u_1 = s + u_F, \tag{3}$$

where s is an axial co-ordinate which is equal to the stretch in the beam along the elastic axis, and u_2 is the transverse deformation, and u_F is the deformation associated with the foreshortening effect, which can be written as

$$u_F = -\frac{1}{2}\int_0^x \left(\frac{\partial u_2}{\partial \xi}\right)^2 \mathrm{d}\xi. \tag{4}$$

The modal assumption method is used for discretization. The axial and transverse deformations are represented by means of the shape function matrices $\boldsymbol{\phi}_1(x)$ and $\boldsymbol{\phi}_2(x)$ as

$$s = \boldsymbol{\phi}_1(x)\mathbf{p}, \quad u_2 = \boldsymbol{\phi}_2(x)\mathbf{p}, \tag{5}$$

where $\mathbf{p}$ is the modal vector.

Substituting Eq. (5) into Eq. (4), one obtains

$$u_1 = \boldsymbol{\phi}_1\mathbf{p} - \tfrac{1}{2}\mathbf{p}^{\mathrm{T}}\mathbf{H}\mathbf{p}, \tag{6}$$

where

$$\mathbf{H} = \int_0^x \left(\frac{\partial \boldsymbol{\phi}_2}{\partial \xi}\right)^{\mathrm{T}} \left(\frac{\partial \boldsymbol{\phi}_2}{\partial \xi}\right) \mathrm{d}\xi. \tag{7}$$

Let $\mathbf{r}$, $\mathbf{r}_0$ be the co-ordinates of $\vec{r}$, $\vec{r}$ with respect to O_0–$X_0Y_0Z_0$, and $\boldsymbol{\rho}'$, $\boldsymbol{\rho}'_0$, $\mathbf{u}'$, be the co-ordinates of $\vec{\rho}$, $\vec{\rho}_0$, $\vec{u}$ with respect to O_1–$X_1Y_1Z_1$, and $\mathbf{A}$ be a matrix transforming a vector of

O_1–$X_1Y_1Z_1$ to O_0–$X_0Y_0Z_0$, which is given by

$$\mathbf{A} = \begin{bmatrix} \cos\theta & -\sin\theta \\ \sin\theta & \cos\theta \end{bmatrix}, \tag{8}$$

then Eq. (1) reads

$$\mathbf{r} = \mathbf{r}_0 + \mathbf{A}\boldsymbol{\rho}', \tag{9}$$

where

$$\boldsymbol{\rho}' = \boldsymbol{\rho}'_0 + \mathbf{u}', \tag{10}$$

$$\boldsymbol{\rho}'_0 = \begin{bmatrix} x \\ 0 \end{bmatrix}, \quad \mathbf{u}' = \begin{bmatrix} u_1 \\ u_2 \end{bmatrix} = \begin{bmatrix} \boldsymbol{\phi}_1 \\ \boldsymbol{\phi}_2 \end{bmatrix} \mathbf{p} - \frac{1}{2} \begin{bmatrix} \mathbf{p}^{\mathrm{T}}\mathbf{H}\mathbf{p} \\ 0 \end{bmatrix}. \tag{11}$$

Differentiating Eq. (9) yields

$$\dot{\mathbf{r}} = \dot{\mathbf{r}}_0 + \dot{\theta}\mathbf{A}\tilde{\mathbf{I}}\boldsymbol{\rho}' + \mathbf{A}\dot{\mathbf{u}}', \tag{12}$$

where

$$\tilde{\mathbf{I}} = \begin{bmatrix} 0 & -1 \\ 1 & 0 \end{bmatrix}, \quad \dot{\mathbf{u}}' = \begin{bmatrix} \boldsymbol{\phi}_1 \\ \boldsymbol{\phi}_2 \end{bmatrix} \dot{\mathbf{p}} - \begin{bmatrix} \mathbf{p}^{\mathrm{T}}\mathbf{H}\dot{\mathbf{p}} \\ 0 \end{bmatrix} \tag{13}$$

and the second differentiation of Eq. (9) leads to

$$\ddot{\mathbf{r}} = \ddot{\mathbf{r}}_0 + \ddot{\theta}\mathbf{A}\tilde{\mathbf{I}}\boldsymbol{\rho}' + \mathbf{A}\ddot{\mathbf{u}}' - \dot{\theta}^2\mathbf{A}\boldsymbol{\rho}' + 2\dot{\theta}\mathbf{A}\tilde{\mathbf{I}}\dot{\mathbf{u}}', \tag{14}$$

where

$$\ddot{\mathbf{u}}' = \begin{bmatrix} \boldsymbol{\phi}_1 \\ \boldsymbol{\phi}_2 \end{bmatrix} \ddot{\mathbf{p}} - \begin{bmatrix} \mathbf{p}^{\mathrm{T}}\mathbf{H}\ddot{\mathbf{p}} \\ 0 \end{bmatrix} - \begin{bmatrix} \dot{\mathbf{p}}^{\mathrm{T}}\mathbf{H}\dot{\mathbf{p}} \\ 0 \end{bmatrix}. \tag{15}$$

4. Virtual work of the elastic force

Using a non-linear strain–displacement relationship, the axial normal strain of an arbitrary point of the beam is expressed as [12]

$$\varepsilon_x = \frac{\partial u_1^*}{\partial x} + \frac{1}{2}\left(\frac{\partial u_2}{\partial x}\right)^2, \tag{16}$$

where

$$u_1^* = u_1 - y\frac{\partial u_2}{\partial x} = s + u_F - y\frac{\partial u_2}{\partial x}. \tag{17}$$

Substituting Eq. (17) into Eq. (16), the axial normal strain can be written as

$$\varepsilon_x = \frac{\partial s}{\partial x} - y\frac{\partial^2 u_2}{\partial x^2} \tag{18}$$

and the virtual work of the elastic force is given by

$$\delta W_f = -\int_V \sigma_x \delta\varepsilon_x \,\mathrm{d}V = -\int_V E\varepsilon_x \delta\varepsilon_x \,\mathrm{d}V$$
$$= -\int_0^l \left[EA\left(\frac{\partial s}{\partial x}\right)\delta\left(\frac{\partial s}{\partial x}\right) + EI\left(\frac{\partial^2 u_2}{\partial x^2}\right)\delta\left(\frac{\partial^2 u_2}{\partial x^2}\right)\right] \mathrm{d}x, \tag{19}$$

where

$$I = \int_A y^2 \,\mathrm{d}A \tag{20}$$

is the area moment of inertia. Substituting Eq. (5) into Eq. (19) yields

$$\delta W_f = -\delta \mathbf{p}^{\mathrm{T}} \mathbf{K}_f \mathbf{p}, \tag{21}$$

where $\mathbf{K}_f$ is the elastic stiffness matrix, which reads

$$\mathbf{K}_f = \int_0^l \left[EA\left(\frac{\partial \boldsymbol{\phi}_1}{\partial x}\right)^{\mathrm{T}}\left(\frac{\partial \boldsymbol{\phi}_1}{\partial x}\right) + EI\left(\frac{\partial^2 \boldsymbol{\phi}_2}{\partial x^2}\right)^{\mathrm{T}}\left(\frac{\partial^2 \boldsymbol{\phi}_2}{\partial x^2}\right)\right] \mathrm{d}x. \tag{22}$$

5. Dynamic equations

The application of the variational procedures gives the principle of virtual work in the form

$$\int_V \delta \mathbf{r}^{\mathrm{T}}(-\rho\ddot{\mathbf{r}} + \mathbf{f}) \,\mathrm{d}V + \delta W_f = 0, \tag{23}$$

where $\mathbf{f} = [f_1 \;\; f_2]^{\mathrm{T}}$ is the body force vector. Substituting Eqs. (9), (14), (21) into Eq. (23) yields

$$\delta \mathbf{q}^{\mathrm{T}}[(\mathbf{M} + \Delta\mathbf{M})\ddot{\mathbf{q}} - (\mathbf{Q} + \Delta\mathbf{Q})] = 0, \tag{24}$$

where $\mathbf{q} = [\mathbf{r}_0^{\mathrm{T}} \;\; \theta \;\; \mathbf{p}^{\mathrm{T}}]^{\mathrm{T}}$ is the generalized co-ordinate of the elastic beam, and $\mathbf{M}$, $\mathbf{Q}$ are the generalized mass and force matrices, and $\Delta\mathbf{M}$, $\Delta\mathbf{Q}$ are the geometric mass and force matrices caused by the inclusion of foreshortening deformation, which can be written as

$$\mathbf{M} = \begin{bmatrix} \mathbf{M}_{rr} & \mathbf{M}_{r\theta} & \mathbf{M}_{rp} \\ \mathbf{M}_{\theta r} & M_{\theta\theta} & \mathbf{M}_{\theta p} \\ \mathbf{M}_{pr} & \mathbf{M}_{p\theta} & \mathbf{M}_{pp} \end{bmatrix}, \quad \mathbf{Q} = \begin{bmatrix} \mathbf{Q}_r \\ Q_\theta \\ \mathbf{Q}_p \end{bmatrix}, \tag{25}$$

$$\mathbf{M}_{rr} = \rho A l \mathbf{I}, \quad \Delta\mathbf{M}_{rr} = 0, \tag{26}$$

$$\mathbf{M}_{\theta r} = \mathbf{M}_{r\theta}^{\mathrm{T}} = [-\mathbf{Y}_2\mathbf{p} \quad E_1 + \mathbf{Y}_1\mathbf{p}]\mathbf{A}^{\mathrm{T}}, \tag{27}$$

$$\Delta\mathbf{M}_{\theta r} = \Delta\mathbf{M}_{r\theta}^{\mathrm{T}} = [0 \quad -\mathbf{p}^{\mathrm{T}}\mathbf{C}\mathbf{p}/2]\mathbf{A}^{\mathrm{T}}, \tag{28}$$

$$\mathbf{M}_{pr} = \mathbf{M}_{rp}^{\mathrm{T}} = [\mathbf{Y}_1^{\mathrm{T}} \quad \mathbf{Y}_2^{\mathrm{T}}]\mathbf{A}^{\mathrm{T}}, \tag{29}$$

$$\Delta\mathbf{M}_{pr} = \Delta\mathbf{M}_{rp}^{\mathrm{T}} = [-\mathbf{C}\mathbf{p} \quad \mathbf{0}]\mathbf{A}^{\mathrm{T}}, \tag{30}$$

$$M_{\theta\theta} = J_{11} + 2\mathbf{Z}_{11}\mathbf{p} + \mathbf{p}^{\mathrm{T}}(\mathbf{W}_{11} + \mathbf{W}_{22})\mathbf{p}, \tag{31}$$

$$\Delta M_{\theta\theta} = -\mathbf{p}^{\mathrm{T}}\mathbf{D}\mathbf{p} - \int_0^l \rho A\mathbf{p}^{\mathrm{T}}\mathbf{H}\mathbf{p}\boldsymbol{\phi}_1\mathbf{p}\,\mathrm{d}x + \frac{1}{4}\int_0^l \rho A\mathbf{p}^{\mathrm{T}}\mathbf{H}\mathbf{p}\mathbf{p}^{\mathrm{T}}\mathbf{H}\mathbf{p}\,\mathrm{d}x, \tag{32}$$

$$\mathbf{M}_{p\theta} = \mathbf{M}_{\theta p}^{\mathrm{T}} = (\mathbf{W}_{21} - \mathbf{W}_{12})\mathbf{p} + \mathbf{Z}_{12}^{\mathrm{T}}, \tag{33}$$

$$\Delta\mathbf{M}_{p\theta} = \Delta\mathbf{M}_{\theta p}^{\mathrm{T}} = \int_0^l \rho A\mathbf{H}\mathbf{p}\boldsymbol{\phi}_2\mathbf{p}\,\mathrm{d}x - \frac{1}{2}\int_0^l \rho A\boldsymbol{\phi}_2^{\mathrm{T}}\mathbf{p}^{\mathrm{T}}\mathbf{H}\mathbf{p}\,\mathrm{d}x, \tag{34}$$

$$\mathbf{M}_{pp} = \mathbf{W}_{11} + \mathbf{W}_{22}, \tag{35}$$

$$\Delta\mathbf{M}_{pp} = -\int_0^l \rho A\boldsymbol{\phi}_1^{\mathrm{T}}\mathbf{p}^{\mathrm{T}}\mathbf{H}\,\mathrm{d}x - \int_0^l \rho A\mathbf{H}\mathbf{p}\boldsymbol{\phi}_1\,\mathrm{d}x + \int_0^l \rho A\mathbf{H}\mathbf{p}\mathbf{p}^{\mathrm{T}}\mathbf{H}\,\mathrm{d}x, \tag{36}$$

$$\mathbf{Q}_r = 2\dot{\theta}\mathbf{A}\begin{bmatrix}\mathbf{Y}_2\dot{\mathbf{p}}\\ -\mathbf{Y}_1\dot{\mathbf{p}}\end{bmatrix} + \dot{\theta}^2\mathbf{A}\begin{bmatrix}E_1 + \mathbf{Y}_1\mathbf{p}\\ \mathbf{Y}_2\mathbf{p}\end{bmatrix} + V\begin{bmatrix}f_1\\ f_2\end{bmatrix}, \tag{37}$$

$$\Delta\mathbf{Q}_r = \mathbf{A}\begin{bmatrix}\dot{\mathbf{p}}^{\mathrm{T}}\mathbf{C}\dot{\mathbf{p}}\\ 0\end{bmatrix} + 2\dot{\theta}\mathbf{A}\begin{bmatrix}0\\ \mathbf{p}^{\mathrm{T}}\mathbf{C}\dot{\mathbf{p}}\end{bmatrix} - \dot{\theta}^2\mathbf{A}\begin{bmatrix}\mathbf{p}^{\mathrm{T}}\mathbf{C}\mathbf{p}/2\\ 0\end{bmatrix}, \tag{38}$$

$$Q_\theta = -2\dot{\theta}[\mathbf{Z}_{11}\dot{\mathbf{p}} + \mathbf{p}^{\mathrm{T}}(\mathbf{W}_{11} + \mathbf{W}_{22})\dot{\mathbf{p}}] + \frac{1}{\rho}[-f_1'\mathbf{Y}_2\mathbf{p} + f_2'(E_1 + \mathbf{Y}_1\mathbf{p})], \tag{39}$$

$$\begin{aligned}\Delta Q_\theta = 2\dot{\theta}\Bigg(&\mathbf{p}^{\mathrm{T}}\mathbf{D}\dot{\mathbf{p}} + \int_0^x \rho A\mathbf{p}^{\mathrm{T}}\boldsymbol{\phi}_1^{\mathrm{T}}\mathbf{p}^{\mathrm{T}}\mathbf{H}\dot{\mathbf{p}}\,\mathrm{d}x + \frac{1}{2}\int_0^x \rho A\mathbf{p}^{\mathrm{T}}\mathbf{H}\mathbf{p}\boldsymbol{\phi}_1\,\mathrm{d}x\dot{\mathbf{p}}\\ &-\frac{1}{2}\int_0^x \rho A\mathbf{p}^{\mathrm{T}}\mathbf{H}\mathbf{p}\mathbf{p}^{\mathrm{T}}\mathbf{H}\dot{\mathbf{p}}\,\mathrm{d}x\Bigg) - \int_0^x \rho A\mathbf{p}^{\mathrm{T}}\boldsymbol{\phi}_2^{\mathrm{T}}\dot{\mathbf{p}}^{\mathrm{T}}\mathbf{H}\dot{\mathbf{p}}\,\mathrm{d}x - \frac{1}{2\rho}f_2'\mathbf{p}^{\mathrm{T}}\mathbf{C}\mathbf{p},\end{aligned} \tag{40}$$

$$\begin{aligned}\mathbf{Q}_p = &-2\dot{\theta}(\mathbf{W}_{21} - \mathbf{W}_{12})\dot{\mathbf{p}} + \dot{\theta}^2\mathbf{Z}_{11}^{\mathrm{T}} - [\mathbf{K}_f - \dot{\theta}^2(\mathbf{W}_{11} + \mathbf{W}_{22})]\mathbf{p}\\ &+\frac{1}{\rho}(f_1'\mathbf{Y}_1^{\mathrm{T}} + f_2'\mathbf{Y}_2^{\mathrm{T}}),\end{aligned} \tag{41}$$

$$\begin{aligned}\Delta\mathbf{Q}_p = &-\dot{\theta}^2\mathbf{D}\mathbf{p} - \dot{\theta}^2\int_0^l \rho A\left(\tfrac{1}{2}\boldsymbol{\phi}_1^{\mathrm{T}}\mathbf{p}^{\mathrm{T}}\mathbf{H}\mathbf{p} - \tfrac{1}{2}\mathbf{H}\mathbf{p}\mathbf{p}^{\mathrm{T}}\mathbf{H}\mathbf{p} + \mathbf{H}\mathbf{p}\boldsymbol{\phi}_1\mathbf{p}\right)\mathrm{d}x\\ &-2\dot{\theta}\int_0^l \rho A(\mathbf{H}\mathbf{p}\boldsymbol{\phi}_2\dot{\mathbf{p}} - \boldsymbol{\phi}_2^{\mathrm{T}}\mathbf{p}^{\mathrm{T}}\mathbf{H}\dot{\mathbf{p}})\,\mathrm{d}x - \frac{1}{\rho}f_1'\mathbf{C}\mathbf{p},\end{aligned} \tag{42}$$

$$\begin{bmatrix}f_1'\\ f_2'\end{bmatrix} = \mathbf{A}^{\mathrm{T}}\begin{bmatrix}f_1\\ f_2\end{bmatrix}, \tag{43}$$

where

$$E_1 = \int_V \rho x\,\mathrm{d}V = \rho A l^2/2, \quad J_{11} = \int_V \rho x^2\,\mathrm{d}V = \rho A l^3/3, \tag{44}$$

$$\mathbf{W}_{mk} = \int_V \rho \boldsymbol{\phi}_m^{\mathrm{T}} \boldsymbol{\phi}_k \, \mathrm{d}V = \int_0^l \rho A \boldsymbol{\phi}_m^{\mathrm{T}} \boldsymbol{\phi}_k \, \mathrm{d}x, \quad m,k = 1,2, \tag{45}$$

$$\mathbf{Y}_k = \int_V \rho \boldsymbol{\phi}_k \, \mathrm{d}V = \int_0^l \rho A \boldsymbol{\phi}_k \, \mathrm{d}x, \quad \mathbf{Z}_{1k} = \int_V \rho x \boldsymbol{\phi}_k \, \mathrm{d}V = \int_0^l \rho A x \boldsymbol{\phi}_k \, \mathrm{d}x, \quad k = 1,2, \tag{46}$$

$$\begin{aligned} \mathbf{C} &= \int_V \rho \mathbf{H} \, \mathrm{d}V = \int_0^l \rho A \left(\int_0^x \left(\frac{\partial \boldsymbol{\phi}_2}{\partial \xi} \right)^{\mathrm{T}} \left(\frac{\partial \boldsymbol{\phi}_2}{\partial \xi} \right) \mathrm{d}\xi \right) \mathrm{d}x \\ &= \int_0^l \rho A \left(\int_\xi^l \left(\frac{\partial \boldsymbol{\phi}_2}{\partial \xi} \right)^{\mathrm{T}} \left(\frac{\partial \boldsymbol{\phi}_2}{\partial \xi} \right) \mathrm{d}x \right) \mathrm{d}\xi = \int_0^l \rho A (l-\xi) \left(\frac{\partial \boldsymbol{\phi}_2}{\partial \xi} \right)^{\mathrm{T}} \left(\frac{\partial \boldsymbol{\phi}_2}{\partial \xi} \right) \mathrm{d}\xi, \end{aligned} \tag{47}$$

$$\begin{aligned} \mathbf{D} &= \int_V \rho x \mathbf{H} \, \mathrm{d}V = \int_0^l \rho A x \left(\int_0^x \left(\frac{\partial \boldsymbol{\phi}_2}{\partial \xi} \right)^{\mathrm{T}} \left(\frac{\partial \boldsymbol{\phi}_2}{\partial \xi} \right) \mathrm{d}\xi \right) \mathrm{d}x \\ &= \int_0^l \rho A \left(\int_\xi^l x \left(\frac{\partial \boldsymbol{\phi}_2}{\partial \xi} \right)^{\mathrm{T}} \left(\frac{\partial \boldsymbol{\phi}_2}{\partial \xi} \right) \mathrm{d}x \right) \mathrm{d}\xi \\ &= \frac{1}{2} \int_0^l \rho A (l^2 - \xi^2) \left(\frac{\partial \boldsymbol{\phi}_2}{\partial \xi} \right)^{\mathrm{T}} \left(\frac{\partial \boldsymbol{\phi}_2}{\partial \xi} \right) \mathrm{d}\xi. \end{aligned} \tag{48}$$

Since $\delta\mathbf{q}$ is arbitrary, the dynamic equations can be written as

$$(\mathbf{M} + \Delta\mathbf{M})\ddot{\mathbf{q}} = \mathbf{Q} + \Delta\mathbf{Q}. \tag{49}$$

In case of prescribed large overall motion with $\ddot{\mathbf{r}}_0' = \mathbf{A}^{\mathrm{T}}\ddot{\mathbf{r}}_0 = [\ddot{x}_0' \;\; \ddot{y}_0']^{\mathrm{T}}$, $\dot{\theta} = \omega$, $\ddot{\theta} = \dot{\omega}$ and $\mathbf{f} = \mathbf{0}$, the equations of motion can be obtained as follows:

$$(\mathbf{M}_{pp} + \Delta\mathbf{M}_{pp})\ddot{\mathbf{p}} + (\mathbf{G} + \Delta\mathbf{G})\dot{\mathbf{p}} + (\mathbf{K} + \Delta\mathbf{K})\mathbf{p} = \mathbf{F} + \Delta\mathbf{F}, \tag{50}$$

where

$$\mathbf{G} = 2\omega(\mathbf{W}_{21} - \mathbf{W}_{12}), \quad \Delta\mathbf{G} = 2\omega \int_0^l \rho A (\mathbf{H}\mathbf{p}\boldsymbol{\phi}_2 - \boldsymbol{\phi}_2^{\mathrm{T}}\mathbf{p}^{\mathrm{T}}\mathbf{H}) \, \mathrm{d}x, \tag{51}$$

$$\mathbf{K} = \mathbf{K}_f - \omega^2(\mathbf{W}_{11} + \mathbf{W}_{22}) + \dot{\omega}(\mathbf{W}_{21} - \mathbf{W}_{12}), \tag{52}$$

$$\Delta\mathbf{K} = \Delta\mathbf{K}_1 + \Delta\mathbf{K}_2, \quad \Delta\mathbf{K}_1 = \omega^2\mathbf{D}, \quad \Delta\mathbf{K}_2 = -\ddot{x}_0'\mathbf{C}, \tag{53}$$

$$\mathbf{F} = \omega^2\mathbf{Z}_{11}^{\mathrm{T}} - \dot{\omega}\mathbf{Z}_{12}^{\mathrm{T}} - \ddot{x}_0'\mathbf{Y}_1^{\mathrm{T}} - \ddot{y}_0'\mathbf{Y}_2^{\mathrm{T}}, \tag{54}$$

$$\Delta\mathbf{F} = -\omega^2 \int_0^l \rho A \left(\tfrac{1}{2}\boldsymbol{\phi}_1^{\mathrm{T}}\mathbf{p}^{\mathrm{T}}\mathbf{H}\mathbf{p} - \tfrac{1}{2}\mathbf{H}\mathbf{p}\mathbf{p}^{\mathrm{T}}\mathbf{H}\mathbf{p} + \mathbf{H}\mathbf{p}\boldsymbol{\phi}_1\mathbf{p} \right) \mathrm{d}x. \tag{55}$$

Eq. (50) shows that $\Delta\mathbf{M}_{pp}$ $\Delta\mathbf{G}$, $\Delta\mathbf{K}$ and $\Delta\mathbf{F}$, which arise from the inclusion of the foreshortening deformation, are all taken into account in the present model. Furthermore, the quadratic and cubic terms of deformation are kept in force expression. However, the inclusion of the high order terms may suffer from the requirement that much computation time is needed.

In case of small deformation, the high order terms of deformation can be ignored, then Eq. (50) is approximated to first order as

$$\mathbf{M}_{pp}\ddot{\mathbf{p}} + \mathbf{G}\dot{\mathbf{p}} + (\mathbf{K} + \Delta\mathbf{K})\mathbf{p} = \mathbf{F}. \tag{56}$$

It is shown that the geometric stiffness matrix $\Delta\mathbf{K}$, which is ignored in conventional modelling methods, is composed of two parts: $\Delta\mathbf{K}_1$ and $\Delta\mathbf{K}_2$. As shown in Eq. (53), $\Delta\mathbf{K}_1$ and $\Delta\mathbf{K}_2$ increase with rotating speed and axial base acceleration growing, therefore, the neglect of $\Delta\mathbf{K}$ may lead to significant error in case of high rotating speed and large base acceleration.

6. Numerical results

In this section, two examples are given in order to demonstrate the geometric stiffening effect on the rigid-flexible coupling dynamics of the elastic beam and to clarify the applicability of the conventional linear model.

(1) *Beam undergoing prescribed translation and rotation*: A cantilever beam attached to a rotating rigid body is shown in Fig. 2. The spin up of the rigid body is given by

$$\omega = \begin{cases} (\Omega/T)[t - (T/2\pi)\sin(2\pi t/T)], & 0 \leqslant t < t_s, \\ \Omega, & t \geqslant t_s. \end{cases} \tag{57}$$

and the acceleration of the beam base is given by

$$\ddot{x}_0' = -\omega^2 b, \quad \ddot{y}_0' = \dot{\omega} b. \tag{58}$$

The properties of the beam are as follows: Mass density $\rho = 2.7667 \times 10^3$ kg/m^3, modulus of elasticity $E = 6.8952 \times 10^{10}$ N/m^2, area moment of inertia $I = 8.219 \times 10^{-9}$ m^4, cross-section area $A = 7.3 \times 10^{-5}$ m^2, and length $l = 8.0$ m.

To illustrate the validity of the first order approximation in case of small deformation, three computer programs are designed. In the first program, all the high order terms of deformation are kept in the dynamic equations, and in the second program, the dynamic equations are approximated to first order, and in the third program, the geometric stiffness matrix $\Delta\mathbf{K}$ is neglected, therefore, the stiffening effect in not taken into account. Finally, the simulation results are compared with the one obtained by Mayo et al. [6]. Gear method is used for integration and

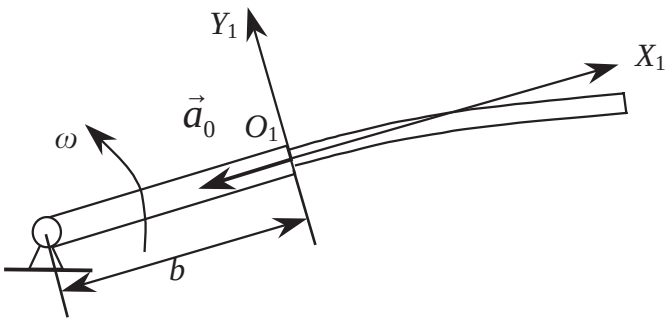

Fig. 2. Beam undergoing prescribed translation and rotation.

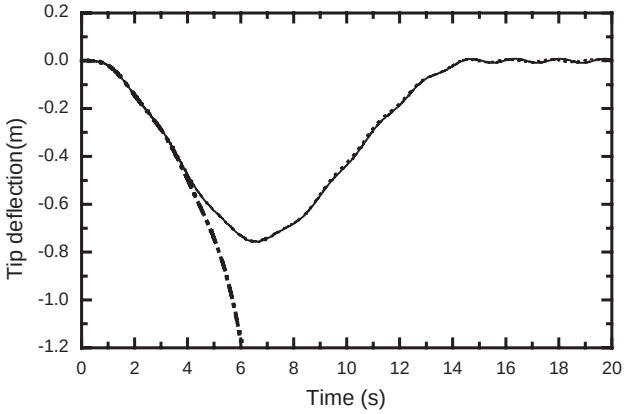

Fig. 3. Tip deflection of the rotating and translating beam: —, high order modelling; - - -, one order modelling; -·-, without stiffening; ..., Mayo [6].

the first three modes of the beam are chosen. The time–history of tip deflection for $\Omega = 6$ rad/s, $T = 15$ s and $b = 0$ are shown in Fig. 3.

As can been seen, there is no significant difference between the results obtained the first and the second program, respectively, and they agree well with Mayo's result. However, the result obtained by the third program shows significant difference. It is demonstrated that the first order Eq. (56) can be used for simulation in case of small deformation and that the geometric stiffness matrix $\Delta\mathbf{K}$ should be taken into account in case of high rotating speed.

For $t \geqslant t_s$, the rotating speed is constant, thus, $\omega = \Omega$, $\dot{\omega} = 0$, and then Eq. (56) reads

$$\mathbf{M}_{pp}\ddot{\mathbf{p}} + \mathbf{G}\dot{\mathbf{p}} + (\mathbf{K} + \Delta\mathbf{K})\mathbf{p} = \omega^2\mathbf{Z}_{11}^{\mathrm{T}} + \omega^2 b\mathbf{Y}_1^{\mathrm{T}}. \tag{59}$$

To illustrate the effect of $\Delta\mathbf{K}$, we define

$$\eta = \omega T, \quad T = \sqrt{\frac{\rho A}{EI}}\, l^2, \tag{60}$$

where η is the dimensionless angular velocity of the beam.

It has been investigated in Ref. [13] that for a slender beam, an accurate solution can be obtained using the first transverse mode without the inclusion of any axial modes in case that $\eta < 3.414$, therefore, the axial deformation can be neglected. Choosing the first transverse mode leads to the simplified dimensionless equation as

$$\frac{\mathrm{d}^2\varsigma}{\mathrm{d}\tau^2} + \eta_{10}^2(1 - 0.08090\eta^2 + 0.09653\eta^2 - 0.1271\xi)\varsigma = 0, \tag{61}$$

where

$$\varsigma = \frac{p}{l}, \quad \tau = \frac{t}{T}, \quad \xi = \frac{\ddot{x}_0' T^2}{l} = -\eta^2\delta, \quad \delta = \frac{b}{l}, \tag{62}$$

are dimensionless modal co-ordinate, time, axial base acceleration and rigid body length, respectively, and η_{10} is the first dimensionless natural frequency of the cantilever beam without

large overall motion, which is given by

$$\eta_{10} = 3.516, \tag{63}$$

and the first dimensionless frequency of the rotating and translating beam with and without geometric stiffening is given by

$$\eta_{1p} = \eta_{10}\sqrt{1 - 0.08090\eta^2 + \underline{0.09653\eta^2 - 0.1271\xi}} \tag{64}$$

and

$$\eta_{1c} = \eta_{10}\sqrt{1 - 0.08090\eta^2}, \tag{65}$$

respectively.

The first dimensionless frequency obtained by the present method is compared with that in Ref. [9]. It is shown that for $\eta = 2$ and $\delta = 0$, $\eta_{1p} = 3.624$ (3.62 in Ref. [9]), and for $\eta = 2$ and $\delta = 1$, $\eta_{1p} = 4.407$ (4.40 in Ref. [9]). Therefore, the results obtained by present model agree well with Ref. [9].

Eqs. (61) and (62) show that the underlined terms lead to different frequency results obtained by the present and conventional models. These terms are related to η and ξ, respectively. In order to reveal the difference between two models, influence ratio c is defined as

$$c = 0.09653\eta^2 - 0.1271\xi = 0.09653\eta^2 + 0.1271\eta^2\delta \tag{66}$$

and relative error of the first frequency of the rotating and translating beam by present and conventional methods is defined as

$$e = (\eta_{1p} - \eta_{1c})/\eta_{1p}, \tag{67}$$

where η_{1p}, η_{1c}, c, e for different η and δ are shown in Figs. 4 and 5.

As shown in Fig. 4, with the rotating speed growing, the first frequency obtained by the conventional linear model decreases rapidly. Furthermore, it is shown that the first frequency obtained by the conventional linear model for $\delta = 0$ (dot line) is well hidden behind that for $\delta = 2$

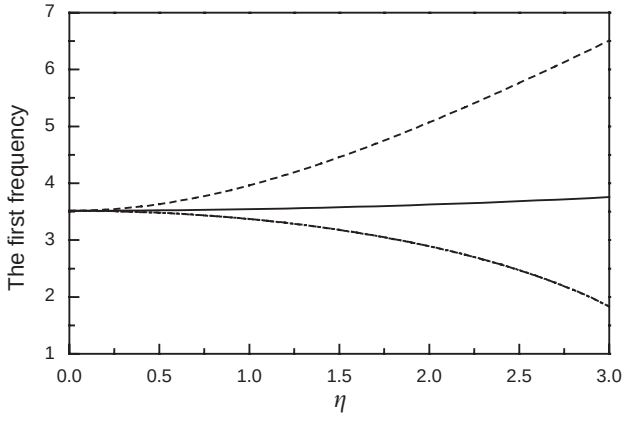

Fig. 4. The first frequency of the rotating and translating beam: —, present modelling ($\delta = 0$); ..., conventional modelling ($\delta = 0$); - - -, present modelling ($\delta = 2$); -·-, conventional modelling ($\delta = 2$).

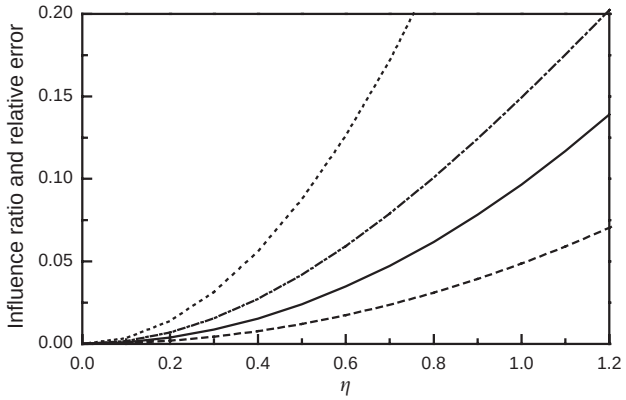

Fig. 5. Influence ratio e and relative error c. —, c ($\delta = 0$); - - -, e ($\delta = 0$); ..., c ($\delta = 2$); -·-, e ($\delta = 2$).

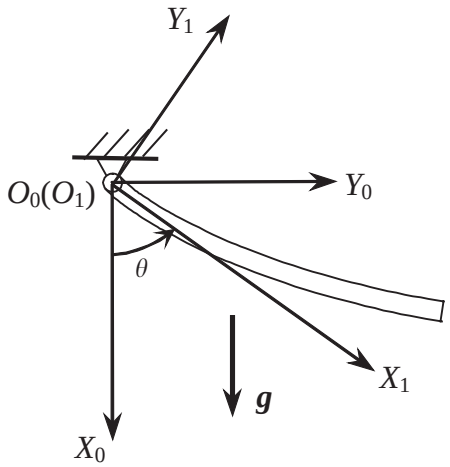

Fig. 6. Single pendulum with gravity.

(dot dash line), it seems that the first frequency has nothing to do with δ. However, the use of the present model leads to different result. It is shown that the first frequency obtained by the present model increases with the rotating speed. Furthermore, it is shown that the increasing rate for $\delta = 2$ is much higher than that for $\delta = 0$ due to the growth of the axial base acceleration.

It is interesting to note in Fig. 5 that for both $\delta = 0$ and 2, e is less than 0.05 in case of $c < 0.1$, and the error arising from the use of the conventional model depends on c instead of η. Since the error is not significant for $e < 0.05$, the conventional linear model can be employed for simulation without any trouble for $c < 0.1$.

(2) *Single pendulum with gravity*: To illustrate the effect of the foreshortening deformation on the large overall motion, the dynamic performance of a single pendulum with free rotation is investigated. The motion of the pendulum is caused by gravity in X_0 direction, as shown in Fig. 6.

Under gravity, the body force vector is

$$\mathbf{f} = \begin{bmatrix} f_1 \\ f_2 \end{bmatrix} = \begin{bmatrix} \rho g \\ 0 \end{bmatrix}, \quad \begin{bmatrix} f_1' \\ f_2' \end{bmatrix} = \mathbf{A}^{\mathrm{T}} \begin{bmatrix} f_1 \\ f_2 \end{bmatrix} = \rho g \begin{bmatrix} \cos\theta \\ -\sin\theta \end{bmatrix}. \tag{68}$$

Since $x_0 = y_0 = 0$, the equations of motion are given by

$$\begin{aligned} (M_{\theta\theta} + \Delta M_{\theta\theta})\ddot{\theta} + (\mathbf{M}_{\theta p} + \Delta\mathbf{M}_{\theta p})\ddot{\mathbf{p}} &= Q_\theta + \Delta Q_\theta, \\ (\mathbf{M}_{p\theta} + \Delta\mathbf{M}_{p\theta})\ddot{\theta} + (\mathbf{M}_{pp} + \Delta\mathbf{M}_{pp})\ddot{\mathbf{p}} &= \mathbf{Q}_p + \Delta\mathbf{Q}_p. \end{aligned} \tag{69}$$

In case of small deformation, the equations can be simplified. With the first order approximation, Eq. (69) can be written as

$$\begin{aligned} &(J_{11} + 2\mathbf{Z}_{11}\mathbf{p})\ddot{\theta} + [\mathbf{p}^{\mathrm{T}}(\mathbf{W}_{21}^{\mathrm{T}} - \mathbf{W}_{12}^{\mathrm{T}}) + \mathbf{Z}_{12}]\ddot{\mathbf{p}} \\ &\quad = -2\dot{\theta}\mathbf{Z}_{11}\dot{\mathbf{p}} + \frac{1}{\rho}[-f_1'\mathbf{Y}_2\mathbf{p} + f_2'(E_1 + \mathbf{Y}_1\mathbf{p})], \\ &[(\mathbf{W}_{21} - \mathbf{W}_{12})\mathbf{p} + \mathbf{Z}_{12}^{\mathrm{T}}]\ddot{\theta} + (\mathbf{W}_{11} + \mathbf{W}_{22})\ddot{\mathbf{p}} \\ &\quad = -[\mathbf{K}_f - \dot{\theta}^2(\mathbf{W}_{11} + \mathbf{W}_{22}) + \dot{\theta}^2\mathbf{D}]\mathbf{p} + \dot{\theta}^2\mathbf{Z}_{11}^{\mathrm{T}} \\ &\qquad - 2\dot{\theta}(\mathbf{W}_{21} - \mathbf{W}_{12})\dot{\mathbf{p}} + \frac{1}{\rho}(f_1'\mathbf{Y}_1^{\mathrm{T}} + f_2'\mathbf{Y}_2^{\mathrm{T}}). \end{aligned} \tag{70}$$

The properties of the beam are given as follows: Mass density $\rho = 2.7667 \times 10^3$ kg/m^3, modulus of elasticity $E = 6.8952 \times 10^{10}$ N/m^2, area moment of inertia $I = 5.0 \times 10^{-9}$ m^4, cross-section area $A = 2.5 \times 10^{-4}$ m^2, and length $l = 2.0$ m.

Gear method is used for integration and the first three modes of the beam are chosen. For $\theta(0) = 90^\circ$, $\dot{\theta}(0) = -15$ rad/s, the simulation is carried out using three different modelling methods: the high order modelling method, the first order modelling method, and the second order conventional modelling method without inclusion of the stiffening terms $\Delta M_{\theta\theta}$, $\Delta\mathbf{M}_{\theta p}$, $\Delta\mathbf{M}_{p\theta}$, $\Delta\mathbf{M}_{pp}$, ΔQ_θ, $\Delta\mathbf{Q}_p$. The time–history of the tip deflection of the beam is shown in Fig. 7, and the angular velocity of the beam is shown in Fig. 8.

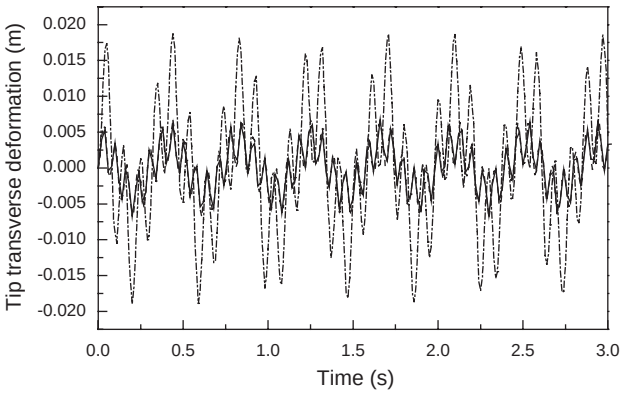

Fig. 7. Tip deflection of the beam for case of $\theta(0) = 90^\circ$, $\omega(0) = -15$ rad/s: —, high-order modelling; - - -, first-order modelling; -·-, without stiffening.

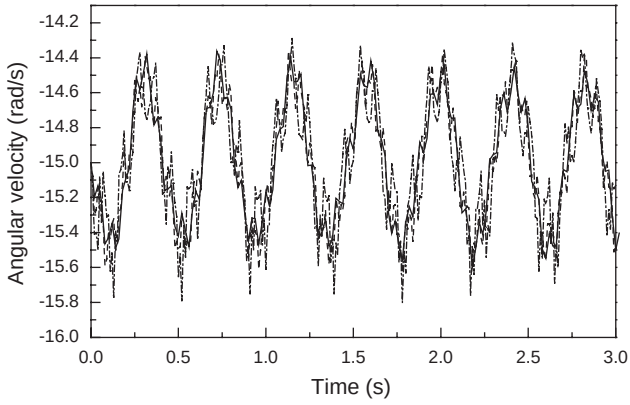

Fig. 8. Angular velocity of the beam for case of $\theta(0) = 90^\circ$, $\omega(0) = -15$ rad/s: —, high-order modelling; - - -, first-order modelling; ---, without stiffening.

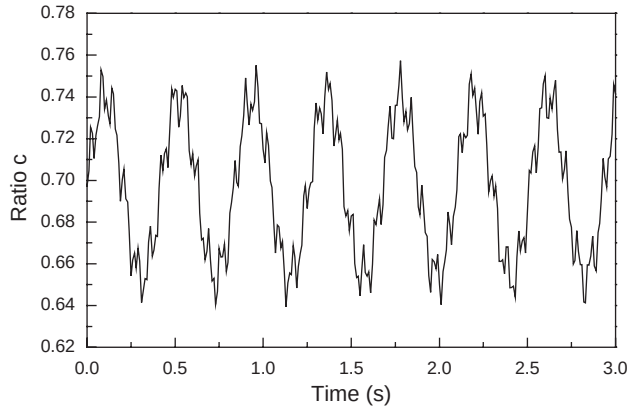

Fig. 9. Ratio c.

It is shown that the results obtained by high order modelling method coincide well with that obtained by first order approximation. However, the neglect of the stiffening terms may lead to significant error.

Since the equations can be approximated to first order in case of small deformation, we can capture the stiffening terms in Eq. (70). It is shown that due to the neglect of the quadratic deformation terms, $\Delta M_{\theta\theta}$, $\Delta\mathbf{M}_{\theta p}$, $\Delta\mathbf{M}_{p\theta}$, $\Delta\mathbf{M}_{pp}$ and ΔQ_θ disappear, therefore, the important stiffening term is

$$\Delta\mathbf{Q}_p = -\dot{\theta}^2\mathbf{D}\mathbf{p}. \tag{71}$$

The influence ratio, which is defined in Eq. (66), is used to illustrate the stiffening effect. Since $\ddot{\mathbf{r}}_0 = \mathbf{0}$, ξ vanishes, thus, the time-varying influence ratio is given by

$$c(t) = 0.09653[\eta(t)]^2 \tag{72}$$

and the time–history of ratio $c(t)$ is shown in Fig. 9.

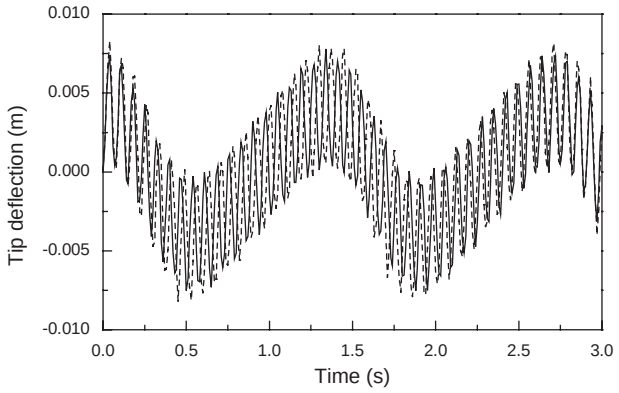

Fig. 10. Tip deflection of the beam for case of $\theta(0) = 90^\circ$, $\omega(0) = -5$ rad/s: —, present modelling; ---, without stiffening.

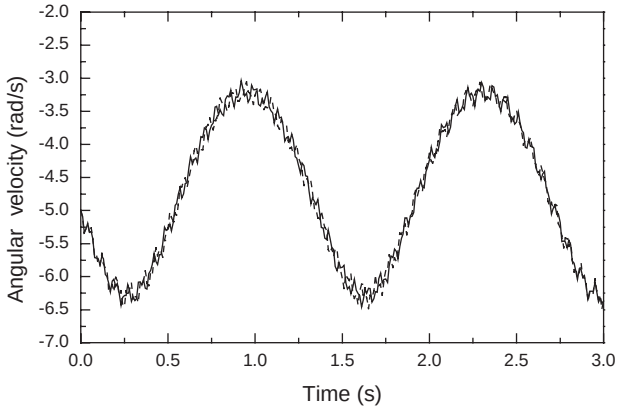

Fig. 11. Angular velocity of the beam for case of $\theta(0) = 90^\circ$, $\omega(0) = -5$ rad/s: —, present modelling; ---, without stiffening.

As can be seen, the minimum value of the ratio is 0.64, which is much high than 0.1. Due to the high ratio, large difference between tip deflections occurs. Since the rotation and deformation are coupled, the angular velocities of the beam with and without stiffening display significant deviation.

In case that the initial angular velocity is reduced to $\omega(0) = -5$ rad/s, Figs. 10 and 11 show little difference in tip deflection and angular velocity. It is revealed that the difference decreases significantly with the angular velocity reducing. The time–history of ratio $c(t)$ is shown in Fig. 12. It is illustrated that in case of $|c(t)| < 0.1$, the foreshortening deformation can be ignored due to the coincidence of the simulation results obtained by the two models.

7. Conclusions

The dynamic performance of a cantilever beam undergoing prescribed translation and rotation is investigated. It is shown that in case of small deformation, the terms of deformation in the

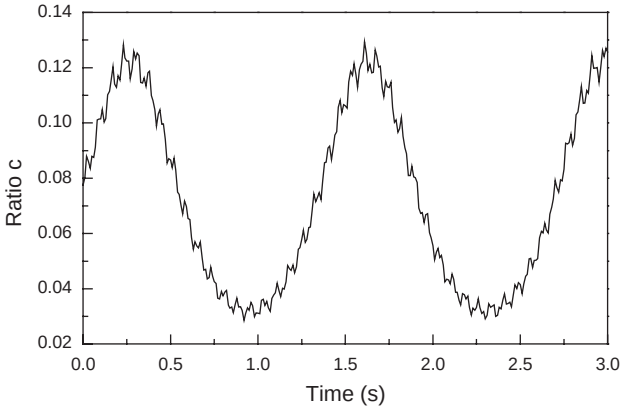

Fig. 12. Ratio c for case of $\theta(0) = 90^\circ$, $\omega(0) = -5$ rad/s.

equation can be approximated to one order. The defined influence ratio c, which is related to the dimensionless axial base acceleration and angular velocity, is used for determination of the application range of the conventional model. According to the relative error of the first frequency of the rotating beam, the application range of the conventional model is clarified. It is shown that the conventional model is suitable in case that the influence ratio c is less than 0.1.

The study on the dynamic stiffening of an elastic beam undergoing prescribed large overall motion is extended to an elastic beam with free large overall motions. The effectiveness of the criterion for the application range of the conventional model is examined. Numerical results for a single pendulum show that the conventional model can be used for $|c(t)| < 0.1$.

Acknowledgements

The research work is supported by the National Science Foundation of China (10372057), for which the authors are grateful.

References

[1] S. Wu, E. Haug, S. Kim, A variational approach to dynamics of flexible multibody system, *Mechanics of Structure and Machine* 17 (1988) 3–32.
[2] J.Z. Hong, *Computational Dynamics of Multibody System*, High Education Press, Beijing, 1999 (in Chinese).
[3] T. Kane, R. Ryan, A. Banerjee, Dynamics of a cantilever beam attached to a moving base, *Journal of Guidance, Control and Dynamics* 10 (1987) 139–151.
[4] J. Simo, L. Vu-Quoc, On the dynamics of flexible beams under large overall motions-the plane case: Part I and II, *Journal of Applied Mechanics* 53 (1986) 849–863.
[5] S. Wu, E. Haug, Geometric non-Linear substructuring for dynamics of flexible mechanical systems, *International Journal for Numerical Methods in Engineering* 26 (1988) 2211–2226.
[6] J. Mayo, J. Dominguez, A. Shabana, Geometrically nonlinear formulation of beams in flexible multibody dynamics, *Journal of Vibration and Acoustics* 117 (1995) 501–509.

[7] J. Mayo, J. Dominguez, Finite element geometrically nonlinear dynamic formulation of flexible multibody systems using a new displacements representation, *Journal of Vibration and Acoustics* 119 (1997) 573–581.
[8] H. Yoo, R. Ryan, R. Scott, Dynamics of flexible beams undergoing large overall motions, *Journal of Sound and Vibration* 181 (1995) 261–278.
[9] H. Yoo, S. Shin, Vibration analysis of rotating cantilever beam, *Journal of Sound and Vibration* 212 (1998) 807–828.
[10] H. Yoo, J. Chung, Dynamics of rectangular plates undergoing prescribed overall motion, *Journal of Sound and Vibration* 239 (2001) 123–137.
[11] J. Ryu, S. Kim, S. Kim, A criterion on inclusion of stress stiffening effect in flexible multibody dynamic system simulation, *Computer and Structures* 62 (1997) 1035–1048.
[12] H. El-Absy, A. Shabana, Geometric stiffness and stability of rigid body modes, *Journal of Sound and Vibration* 207 (1997) 465–496.
[13] J.Y. Liu, Study on Dynamic Modeling Theory of Rigid-Flexible Coupling Systems, Ph.D. Dissertation, Shanghai Jiao Tong University, Shanghai, 2000 (in Chinese).